

## Diffusion through Porous Media: Ultrafiltration, Membrane Permeation and Molecular Sieving

*Douglas M. Ruthven*

Dept. of Chemical Engineering, University of Maine, Orono,  
ME 04469, U.S.A.

Corresponding author:  
Douglas M. Ruthven  
Dept. of Chemical Engineering  
University of Maine  
ME 04469, Orono, U.S.A.  
E-Mail: DRuthven@umche.maine.edu

### Abstract

This paper considers permeation through microporous or nanoporous inorganic membranes under the influence of an applied pressure gradient. In general membrane permeation may be considered as a diffusive process, driven by the gradient of chemical potential (which depends on both composition and pressure). The relative importance of these two factors varies greatly for different types of system. The general features of such processes are reviewed and the diffusional behavior of selected systems is examined.

(membrane permeation, osmosis, diffusion, zeolite membrane, DDR-3, SAPO-34)

### 1. Introduction

The permeation of gases and liquids through microporous membranes has been studied for many years. The first commercial application as a large scale separation process, introduced in the 1960s, was the desalination of brackish water by reverse osmosis (RO) using a cellulose acetate membrane, which selectively retains the salt allowing pure water to permeate<sup>(1)</sup>. As new membrane materials became available more sophisticated applications of RO and ultrafiltration were developed and in recent years many membrane processes for gas separation have followed. Most of the established processes use polymeric membranes but in the last decade, stimulated by the discovery of ordered microporous silicas<sup>(2,3)</sup> and the ability to grow coherent layers of crystalline zeolites<sup>(4)</sup>, the potential of inorganic (ceramic) membranes has attracted much attention. Membrane permeation depends on diffusion but the nature of the diffusion process depends on many factors including the phase of the system, the pore size, the size of the permeating molecules and the driving force. Selected examples drawn from several different types of membrane system are presented in order to illustrate some of the different mechanisms and the resulting patterns of behavior. The focus of this paper is on inorganic membranes, reflecting the interests of the author, even though such systems comprise only a small fraction of membrane technology.

## 2. Ultrafiltration and Reverse Osmosis

In most membrane processes the flux through the membrane is driven by a pressure difference applied across the membrane. The fundamental driving force for transport through the membrane is the gradient of chemical potential but, in many situations, the pressure gradient induces an equivalent gradient of concentration, so the flux may be regarded as diffusion down the concentration gradient. The distinctive feature of RO and ultrafiltration is that the preferentially permeating species, the solvent, diffuses *up* the gradient of concentration, driven by the effect of pressure on the chemical potential. Such processes are generally modeled by either the “solution - diffusion” or the “pore flow” model<sup>(5,6)</sup>. In the standard development the former model postulates step changes in pressure and solvent activity at the low pressure interface while the latter model postulates step changes at the high pressure surface. For the “solution – diffusion” model this may be physically reasonable in view of the change in phase but for the pore flow model such an assumption seems untenable. This difficulty is easily avoided by considering the effect of pressure on the chemical potential within the membrane, which is not allowed for in the standard treatment of the pore flow model.

### Mathematical Model

Neglecting mutual diffusion effects, the flux is given by:

$$N_i = -\frac{D_{oi}c_i}{RT} \cdot \frac{d\mu_i}{dz} \quad (1)$$

$$\mu_i = \mu_i^o + RT \ln(\gamma_i x_i); \quad \frac{\partial \mu_i^o}{\partial P} = v_i \quad (2)$$

For a thermodynamically ideal system:

$$\frac{d\mu_i}{dz} = RT \frac{d \ln x_i}{dz} + v_i \frac{dP}{dz} \quad (3)$$

Combining with Eq.1 and integrating across the membrane (from  $z = 0$ ,  $X_i = X_{i0}$  to  $z = \ell$ ,  $X_i = X_{i\ell}$ ) yields, for the concentration profile:

$$A \frac{X_i}{X_{i0}} = 1 - (1 - A) \exp\left[\frac{v_i \Delta P}{RT} \cdot \frac{z}{\ell}\right] \quad (4)$$

where  $\Delta P = P_o - P_t$  and  $A = \frac{v_i \Delta P}{RT} \cdot \frac{D_{oi} c_{oi}}{N_i \ell}$ . The flux is given by:

$$\frac{N_i \ell}{D_{oi} c_i} = \frac{v_i \Delta P}{RT} \frac{X_{i0} e^{\frac{v_i \Delta P}{RT}} - X_{i\ell}}{e^{\frac{v_i \Delta P}{RT}} - 1} = \frac{a_i [X_{i0} e^{a_i} - X_{i\ell}]}{e^{a_i} - 1} \quad (5)$$

If the flux is zero we have:

$$\frac{X_{i\ell}}{X_{i0}} = \exp\left(\frac{v_i \Delta P}{RT}\right) \quad (6)$$

where  $\Delta P = \Delta \pi$ , the difference in osmotic pressure between the solution and the permeate. If  $\frac{v_i \Delta P}{RT} \ll 1$ , Eq 5 reduces to:

$$\frac{v_i \Delta P}{RT}$$

$$\frac{N_i \ell}{D_{oi} c_i X_{i0}} \approx \exp\left(\frac{v_i \Delta P}{RT}\right) - \exp\left(\frac{v_i \Delta \pi}{RT}\right) \approx \frac{v_i}{RT} (\Delta P - \Delta \pi) \quad (7)$$

which is the commonly used design equation for RO processes<sup>(7)</sup>. The major point that emerges from this derivation is that Eq 7 is a valid approximation only when the condition  $v_i \Delta P / RT \ll 1$  is fulfilled. This limitation is not obvious from the derivation commonly given in elementary textbooks.

At the other extreme, when  $v_i \Delta P / RT \gg 1$  and  $X_{i0} \approx 1$  Eq 5 reduces to:

$$N_i \approx \frac{D_{oi} c_{i0}}{\ell} \frac{v_i \Delta P}{RT} \approx \Pi \frac{\Delta P}{\ell} \quad (8)$$

where  $\Pi$  is the “permeability”.

This is the basic expression for ultrafiltration. Ultrafiltration and RO are similar processes but the distinction is that in ultrafiltration the molecular weight of the solute (or the mass of the colloidal particle) is so large that the activity of the solvent is always very close to unity so that the osmotic pressure is negligible and the flux is directly proportional to the pressure gradient.

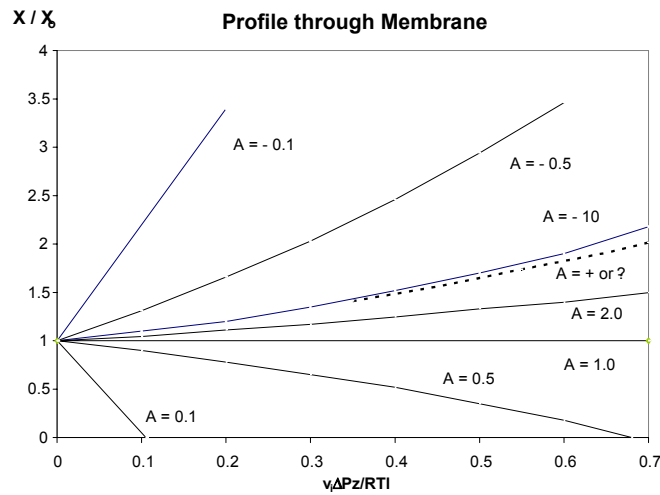


Fig. 1: Concentration profiles through the membrane. The plot shows the normalized concentration of component  $i$  ( $X_i / X_{i0}$ ) plotted against the distance coordinate

$$\left(\frac{v_i \Delta P z}{RT \ell}\right) \text{ for various values of the parameter } A = \left(\frac{D_{oi} c_{i0}}{N_i \ell} \frac{v_i \Delta P}{RT}\right).$$

#### Profiles and Fluxes

Figure 1 shows the concentration profile through the membrane for various values of the parameter  $A$ , calculated from Eq. 4. The sign of this parameter depends on the sign of  $\Delta P / N_i$ . If  $X_{i0} / X_{i0}$  we have a pressure driven flow against the concentration gradient. A positive value of  $A$  corresponds to the situation in which the flux of  $i$  is in the direction of

the pressure gradient (and against the concentration gradient) while a negative value of  $A$  corresponds to the situation where the flux is in the opposite direction (against the pressure gradient but down the concentration gradient) from the permeate to retentate sides of the membrane. The limiting curve for  $A \rightarrow \pm\infty$  corresponds to osmotic equilibrium ( $N_i = 0$ ).

The horizontal line for  $A = 1$  corresponds to the situation in which there is no change in composition through the membrane, as in ultrafiltration. In contrast to the “solution – diffusion” model, which predicts linear profiles and the classical “pore flow” model, which predicts a constant concentration through the membrane with a step change at  $z = 0$ , the profiles are in general curved.

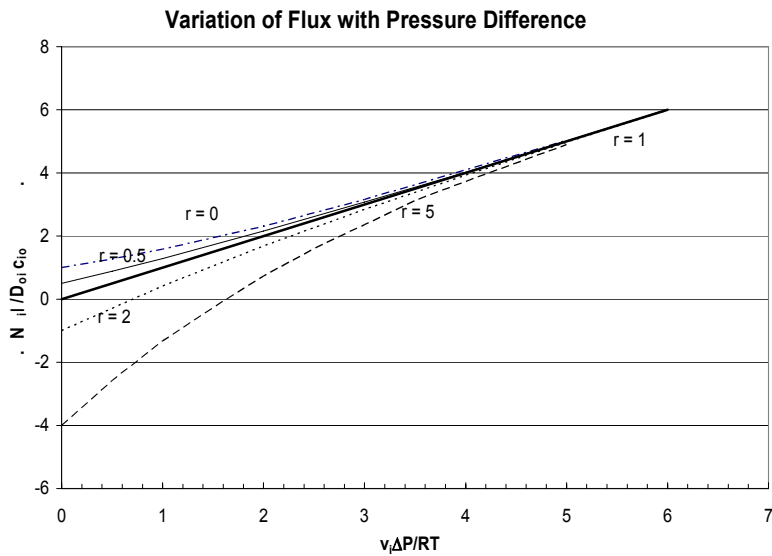


Fig. 2: Variation of the normalized flux ( $N_i l / D_{oi} C_{i0}$ ) with parameter  $a$ .

Figure 2 shows the variation of flux with the dimensionless pressure difference ( $v_i \Delta P / RT$ ) for three different values of the concentration ratio ( $r = X_{it} / X_{i0}$ ). The intercept on the  $x$  axis corresponds to the dimensionless osmotic pressure ( $v_i \Delta \pi / RT$ ). The variation of flux with pressure difference is linear only when  $r \rightarrow 1$  (ultrafiltration) but, except when the change in concentration is large, the curvature is relatively small.

### Selectivity

An expression for the separation factor ( $\alpha_{ij}$ ) may be derived by considering the ratio of the fluxes for the two components ( $i, j$ ) in a binary solution:

$$\alpha_{ij} = \frac{X_{i\ell} X_{j0}}{X_{i0} X_{j\ell}} = \frac{D_{i0} a_i (e^{a_i} - X_{i\ell} / X_{i0}) (e^{a_j} - 1)}{D_{j0} a_j (e^{a_j} - X_{j\ell} / X_{j0}) (e^{a_i} - 1)} \quad (9)$$

where  $a_i = v_i \Delta P / RT$ . For a specified feed composition ( $X_{i0}$ ,  $X_{j0} = 1 - X_{i0}$ ), diffusivity ratio and volume ratio this equation may be solved to obtain the effluent composition ( $X_{i\ell}$ ,  $X_{j\ell}$ ), and hence the separation factor, as a function of  $a_i$  (the dimensionless pressure difference).

When the molar volumes are equal ( $a_i = a_j = a$ ) Eq. 9 reduces to:

$$\alpha_{ij} = \frac{D_{i0}}{D_{j0}} \left( \frac{e^a - X_{i\ell} / X_{i0}}{e^a - X_{j\ell} / X_{j0}} \right) \quad (10)$$

and in the high pressure limit ( $a_i$  and  $a_j$  both large) Eq. 9 reduces to:

$$\alpha_{ij} = \frac{D_{i0} a_i}{D_{j0} a_j} = \frac{D_{i0} v_i}{D_{j0} v_j} \quad (11)$$

showing that the limiting value of the separation factor corresponds to the product of the diffusivity and molecular volume ratio. If  $a_i$  and  $a_j$  are both small Eq. 9 becomes:

$$\alpha_{ij} = \frac{D_{i0}}{D_{j0}} \frac{(e^{a_i} - X_{i\ell} / X_{i0})}{(e^{a_j} - X_{j\ell} / X_{j0})} \quad (12)$$

and if the solution is dilute ( $X_{i0} \rightarrow 1$ ) and the diffusivity ratio large enough to ensure  $X_{j\ell} \rightarrow 0$  this reduces further to:

$$\frac{\alpha_{ij}}{D_{i0} / D_{j0}} \approx \frac{v_i}{RT} (\Delta P - \Delta \pi) \quad (13)$$

showing that, in this limit, the separation factor becomes independent of  $v_j$ .

When the solution is more concentrated and for larger pressure differences the separation factor becomes dependent on the composition (as well as on the molar volumes of both components). The pattern of behavior is illustrated in figure 3. In general the separation factor increases with pressure difference. Even if there is no difference in diffusivity it is still possible to achieve a separation on the basis of the difference in molecular volumes (Eq.11) although this is seldom of practical interest since the ratio of molecular volumes is generally not large enough to yield sufficient selectivity. If  $a_i/a_j > 1$ , the separation factor will be greater than the diffusivity ratio but if  $a_i/a_j < 1$ , then the separation factor will be lower than the diffusivity ratio. For both cases the high pressure limit is given by Eq.11. This means that, in the former case, the performance can be improved by increasing the pressure. However, that will only occur when the larger molecule has the higher diffusivity. More commonly the larger molecule has the lower diffusivity and, in that case, the advantage of raising the pressure is less pronounced.

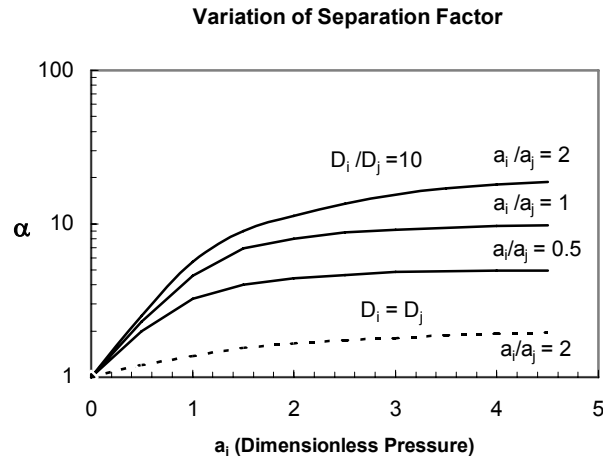


Fig. 3: Variation of separation factor ( $\alpha_{ij}$ ) with dimensionless pressure ( $a_i$ ). The curves are calculated from Eq.9 for various values of the diffusivity ratio and volume ratio. In all cases  $X_{i0} = 0.5$

#### Mutual Diffusion Effects

The simplified formulation of the transport equations which is used here makes no allowance for mutual diffusion effects (i.e. the tendency of the faster diffusing species to “drag” the slower species with it and *vice versa*). Such effects, which may be quite important, are best accounted for in terms of the Maxwell –Stefan model (see Eq. 17 below). The modified analysis is summarized in the appendix. It turns out that the diffusional resistance is modified (and the definition of the parameter  $a$  must be changed but the general form of the expressions for the flux and concentration profile are not altered.

### 3. Mesoporous Silica Membranes

Since their discovery in 1992<sup>(2)</sup>, several different families of ordered mesoporous silicas have been synthesized and characterized. The potential for application of these materials as inorganic membranes with a uniform pore size was quickly recognized and a good deal of research has been directed to their preparation in membrane form. The pore diameter is quite uniform and typically in the range 40 – 100 nm. Without further modification such membranes can be used for ultrafiltration of colloids and large biomolecules<sup>(8,9)</sup>. However, they are not useful for gas separation since, in pores of this size (at ordinary pressures) transport occurs mainly by Knudsen diffusion, leading to very modest selectivities.

From recent theoretical modeling studies and molecular simulations<sup>(10-14)</sup> it has been suggested that the Knudsen model over-predicts the diffusivity by as much as an order of magnitude, for light gas molecules that are significantly adsorbed. However, the

results of an experimental study carried out in our laboratory<sup>(15,16)</sup> do not support such a conclusion.

#### *Permeance Measurements*

In modelling permeation through this type of membrane it is essential to allow for the mass transfer resistance of both the support and the active layer. Since the pores of the support are very much larger we assume viscous flow through the support with Knudsen diffusion, possibly augmented by surface diffusion, through the active layer. Using the principle of additivity of resistances the overall permeance ( $\pi$ ) is therefore given by:

$$\frac{1}{\pi\mu RT} = \frac{z}{\mu D_e} + \left(\frac{\tau^1 z^1}{\varepsilon^1}\right) \frac{8}{\bar{P}a^2} \quad (14)$$

where  $D_e$  represents the “effective” Knudsen diffusivity ( $D_e = \varepsilon D_K/\tau$ ). According to the Knudsen model  $D_K = 97r\sqrt{T/M}$  ( $\text{m}^2\cdot\text{s}^{-1}$ ) so Eq. 14 becomes:

$$\frac{1}{\pi\mu RT} = \left(\frac{\tau z}{\varepsilon r}\right) \cdot \frac{1}{97\mu} \cdot \sqrt{\frac{M}{T}} + \left(\frac{\tau^1 z^1}{\varepsilon^1}\right) \frac{8}{\bar{P}a^2} \quad (15)$$

The second term on the right hand side of Eq. 15, representing the resistance of the support, is constant, so if the Knudsen model is valid with no significant surface flow contribution, a plot of the experimental permeance data in the form  $1/(\pi\mu RT)$  vs  $1/(\mu\sqrt{T/M})$  should yield a straight line with slope  $\tau z/97\varepsilon r$  and intercept  $8\tau^1 z^1 / \varepsilon^1 \bar{P}a^2$  (the support resistance). Representative experimental data for the permeation of several light gases through a typical mesoporous silica membranes are plotted in this way in figure 4. It is evident that Eq. 15 provides a good representation of the data with no evidence of any systematic deviation from the simple Knudsen model. From the slope of figure 4 we find  $(\varepsilon r/\tau z) = 1.02 \times 10^{-5}$ . With  $r \approx 2.8$  nm and  $\varepsilon \approx 0.12$  from porosimetry measurements and  $z = 10$   $\mu\text{m}$ , estimated from an electron micrograph of the membrane cross section, we find  $\tau \approx 3.2$ , an eminently reasonable value for the tortuosity factor.

The functional dependence of the pore diffusivity on  $\sqrt{(T/M)}$ , as predicted by the Knudsen model, is confirmed by the experimental data and, although the estimates of porosity and pore size are subject to some uncertainty, the quantitative prediction [ $D = 97r\sqrt{(T/M)}$ ] also appears to be valid, at least approximately. It is noteworthy that, under the experimental conditions He is not adsorbed (to any measurable extent) whereas the other gases, especially propane, are significantly adsorbed, yet the permeance data for all species lie close to the same line (in figure 4), implying that, in contrast to the conclusions drawn from the molecular simulations, the validity of the Knudsen model is not significantly affected by at least a modest degree of adsorption. Very similar conclusions were reached by Markovic et al.<sup>(62)</sup> from a recent study of permeation through porous glass membranes of similar pore size.

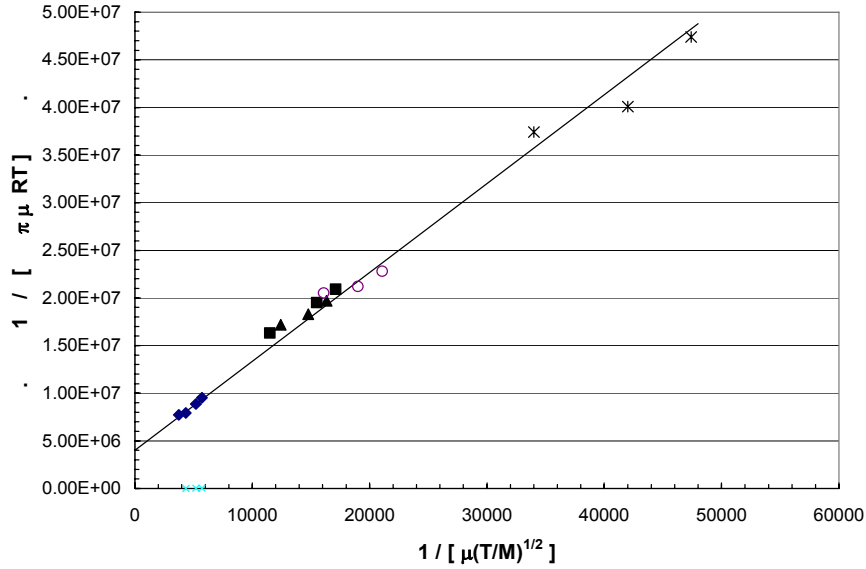


Fig. 4. Experimental permeance data for light gases through a mesoporous silica membrane plotted as  $1/(\pi\mu RT)$  vs  $1/(\mu\sqrt{T/M})$  in accordance with Eq.15 (He,  $\blacklozenge$ ;  $N_2$ ,  $\blacksquare$ ; Ar,  $\blacktriangle$ ;  $CH_4$ ,  $\circ$ ;  $C_3H_8$ ,  $*$ )<sup>(16)</sup>. Units are given in the notation.

#### Modified Mesoporous Silica Membranes<sup>(15)</sup>

There have been numerous attempts to make mesoporous membranes more selective for gas separation by modification of the pore surface. Since the silica surface contains hydroxyls which are quite reactive, many different modifications can be easily achieved<sup>(17-24)</sup>. In our experimental studies mesoporous silica membranes similar to that discussed above were silanated using triethylamine and octadecyl-dimethylchlorosilane with supercritical  $CO_2$  as the solvent<sup>(25)</sup> to yield a structure in which, after pre-conditioning, the internal surface is covered with tethered  $C_{18}$  alkane chains, attached in place of the surface hydroxyls. The resulting membranes showed significantly reduced permeance (by a factor of about 5), in comparison with the unmodified membranes, so that the support resistance was no longer significant.

According to the Knudsen model, in the absence of support resistance, the permeance should be given by:

$$\pi \left( \frac{\text{mol}}{\text{m}^2 \cdot \text{s} \cdot \text{Pa}} \right) \approx \frac{97}{R} \left( \frac{\varepsilon r}{\tau z} \right) \frac{1}{\sqrt{TM}} \quad (16)$$

The experimental permeance data showed the  $1/\sqrt{M}$  dependence predicted by the Knudsen model but the temperature dependence was much stronger, approximating  $1/T^2$  rather than  $1/\sqrt{T}$ , as may be seen from figure 5. This implies that the parameter  $(\varepsilon r/\tau z)$  decreases with temperature as shown in figure 6.

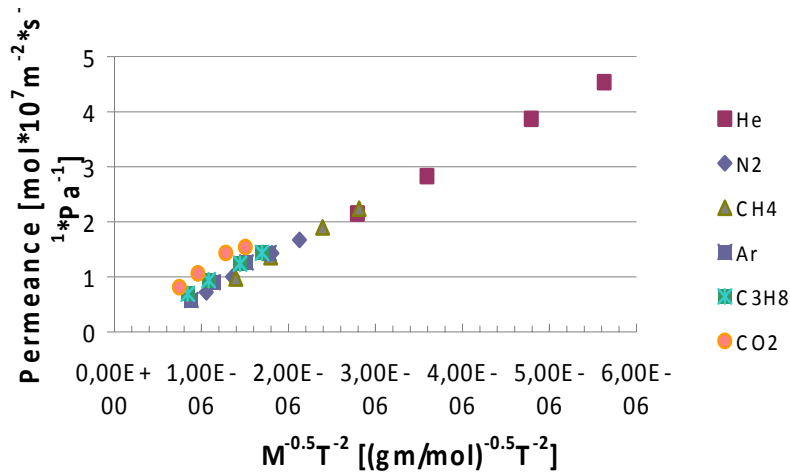


Fig. 5: Plot of permeance ( $\pi$ ) vs.  $\frac{1}{M^{0.5}T^2}$  for modified Membrane B. (from Higgins et al.<sup>(15)</sup>).

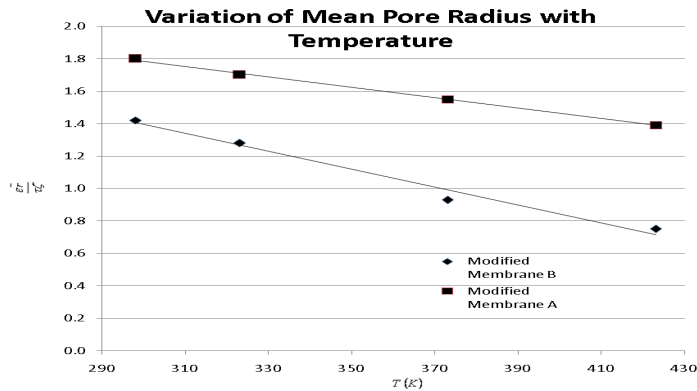


Fig. 6: Variation of parameter  $\frac{\bar{\epsilon}T}{\tau z}$  with temperature for the modified membranes calculated by

matching the permeance data to Eq.16 (Higgins et al.<sup>(15)</sup>).

Despite the substantial reduction in permeance the selectivity of the modified membranes did not differ significantly from the Knudsen value (the square root of the molecular weight ratio) – see Table 1. The only significant exception was CO<sub>2</sub>, which diffused somewhat faster than expected (on the basis of molecular weight) in the modified membrane. As a result the permeability ratio for CO<sub>2</sub>/C<sub>3</sub>H<sub>8</sub> ( $M = 44$  for both species) shows a modest selectivity ( $\approx 1.3$ ) and the permeability ratio for CH<sub>4</sub>/CO<sub>2</sub> shows a reduced selectivity (1.1 – 1.2) in comparison with the Knudsen value (1.66). These results were confirmed by both single component and binary mixture measurements which were quite consistent (see Table 2).

**Table 1: Permeance Ratios Calculated from Single Component Data<sup>(15)</sup>**

Sorbates (1,2)	$\sqrt{M_2/M_1}$	$(\pi_1/\pi_2)_{Av.}$		% Deviation
		Membrane A	Membrane B	
He/CH <sub>4</sub>	2.0	2.24	2.22	+10
He/N <sub>2</sub>	2.65	2.89	2.84	-7.4
He/Ar	3.16	3.26	3.46	+6.3
He/C <sub>3</sub> H <sub>8</sub>	3.32	3.14	3.30	-3.0
He/CO <sub>2</sub>	3.32	2.38	2.65	-25
CO <sub>2</sub> /C <sub>3</sub> H <sub>8</sub>	1.0	1.32	1.25	+28
CH <sub>4</sub> /CO <sub>2</sub>	1.66	1.06	1.19	-30

**Table 2: Comparison of Single Component and Binary Permeance Data at 373K<sup>(15)</sup>**  
Single Component Data

	Permeance (mol/m <sup>2</sup> · s · Pa)		
	Membrane A	Membrane B	Membrane D
CH <sub>4</sub>	2.02 x 10 <sup>-7</sup>	1.36 x 10 <sup>-7</sup>	2.39 x 10 <sup>-8</sup>
CO <sub>2</sub>	1.85 x 10 <sup>-7</sup>	1.07 x 10 <sup>-7</sup>	2.25x 10 <sup>-8</sup>
	Binary Data – Permeance Ratio		
CH <sub>4</sub> /CO <sub>2</sub>	1.07 (1.09)	(1.27)	1.19 (1.06)
N <sub>2</sub> /C <sub>3</sub> H <sub>8</sub>	(1.085)	(1.16)	1.17

Values calculated from single component permeances are in brackets.

If it is assumed that the modification procedure changes only the pore radius, without affecting the membrane thickness or tortuosity, the parameter ( $\epsilon r/\tau z$ ) will be proportional to  $r^3$  (since  $\epsilon$  is proportional to  $r^2$ ). The permeance data therefore suggest that the effective pore radius of the modified membranes is about 1.5 nm (compared with 2.7 nm for the unmodified membranes). This is evidently still too large for substantial steric hindrance but the enhanced temperature dependence and the anomalous behavior of CO<sub>2</sub> in the modified membranes show that the diffusion mechanism is clearly modified to some extent.

#### 4. Molecular Sieve Membranes for Gas Separation

The possibility of separating gases by size selective molecular sieving in microporous solids was demonstrated by McBain more than 70 years ago<sup>(26)</sup> and the potential use of zeolites in this context was explored in considerable detail by Professor R.M. Barrer and his students in a series of 400 papers spanning more than 50 years (1934 – 1993)<sup>(27)</sup>. The structural regularity and uniformity of pore size make the zeolites prime

candidates for molecular sieve membranes and laboratory scale tests have shown that, for several practically important separations (e.g. CO<sub>2</sub>/CH<sub>4</sub>, C<sub>3</sub>H<sub>6</sub>/C<sub>3</sub>H<sub>8</sub>), the performance of zeolite membranes substantially exceeds that of the best polymeric membranes (see Table 3). However, the difficulties associated with producing a robust and coherent zeolite membrane have hindered the commercial development of such processes<sup>(39)</sup>.

**Table 3: Performance of Membranes for CO<sub>2</sub>/CH<sub>4</sub> Separation**

Membrane Type	CO <sub>2</sub> Permeance (mol/m <sup>2</sup> .s.Pa)	$\alpha_{\text{CO}_2/\text{CH}_4}$	Reference
<b><i>Zeolite membranes</i></b>			
DDR on $\alpha$ -alumina	$3 \times 10^{-7}$	400	Himeno <sup>(31)</sup>
DDR on $\alpha$ -alumina Bergh <sup>(32)</sup>	$7 \times 10^{-8}$	600	van den
SAPO-34 on $\alpha$ -alumina Li <sup>(34)</sup>	$10^{-7}$ - $10^{-6}$	65 – 170	Carreon <sup>(33)</sup> ,
<b><i>Polymeric Membranes</i></b>			
Polyimides	$0.6 - 4 \times 10^{-10}$	10 – 80	Sridhar <sup>(35)</sup>
Polycarbonate	$1 \times 10^{-9}$	100 – 150	Iqbal <sup>(36)</sup>
Polyallyl imide –			
Poly(vinyl alcohol/polysulfone)	$10^{-8}$	60	Cai <sup>(37)</sup>
Polyurethane/PVA blends	$10^{-10}$	50	Ghalen <sup>(38)</sup>

There are two different separation mechanisms: selective surface flow and size selective sieving. In the former mechanism the more strongly adsorbed species (usually the larger molecule) excludes the less strongly adsorbed species from the pore structure by competitive adsorption, leading to preferential permeation of the larger molecule<sup>(28-30)</sup>. The maximum selectivity is however limited by entropic effects which prohibit the total exclusion of the smaller species. The latter mechanism depends simply on size exclusion of the larger molecule, leading to preferential permeation of the smaller species. In principle, with a perfect membrane, the selectivity can be infinite.

### Correlation of Diffusivity with Minimum Window Diameter

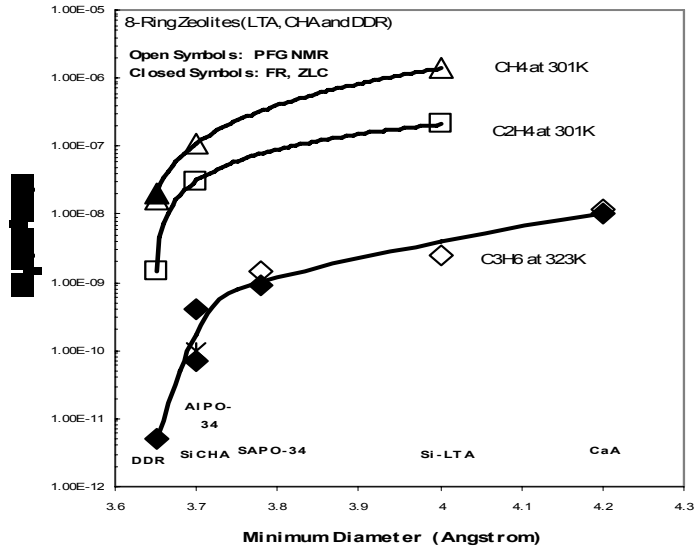


Fig. 7: Correlation of intracrystalline diffusivity with minimum window aperture. (Data are from a variety of sources including Reyes et al.<sup>(40-42)</sup> and ZLC data from this laboratory.)

#### The Maxwell–Stefan Model

The most successful approach to the modeling of permeation in zeolite membranes is based on the Maxwell–Stefan model, which postulates that the flux is driven by the gradient of chemical potential and the diffusional resistance can be considered as the sum of the drag due to interaction of the diffusing molecules with the pore wall and the interference between the different types of diffusing molecules. For diffusion of a binary mixture, the fluxes ( $N_i$  and  $N_j$ ) are given by:

$$-\frac{q_i}{RT} \frac{d\mu_i}{dz} = \frac{q_j N_i - q_i N_j}{q_s \bar{D}_{ij}} + \frac{N_i}{D_{oi}} \quad (17)$$

with a similar expression for  $N_j$ .  $D_{oi}$  and  $D_{oj}$  represent the thermodynamically corrected diffusivities of components  $i$  and  $j$  (as in Eq. 1 for single component diffusion) while  $\bar{D}_{ij}$  represents the mutual diffusivity. The main advantage of this approach is that it is possible to estimate these diffusivities from single component data. The procedures have been developed by Krishna and his coworkers in a series of papers<sup>(43-53)</sup>. A good example of the application of this model to a zeolite membrane is the paper by van de Graaf et al. which reports the successful prediction of binary behavior from single component data for the system  $\text{CH}_4\text{-C}_2\text{H}_6/\text{silicalite}$ <sup>(54)</sup>.

When mutual diffusion effects are insignificant ( $\mathcal{D}_{ij} \rightarrow \infty$ ) Eq. 17 reduces to Eq.1 and the components in the mixture diffuse independently, although the fluxes are still coupled through the binary isotherm (since  $\mu_i$  depends on the concentrations of both components). This is the ‘‘Habgood model’’ which was the first reasonable model to represent diffusion in a binary system<sup>(55,56)</sup>.

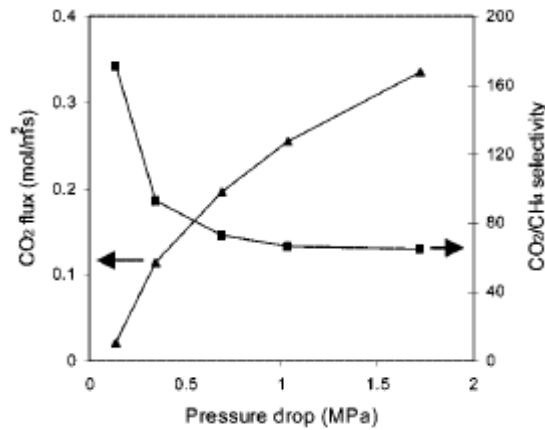


Fig. 8: Variation of CO<sub>2</sub> flux and CO<sub>2</sub>/ CH<sub>4</sub> selectivity with pressure drop for a SAPO-34 membrane. From Carreon et al.<sup>(33)</sup>.

#### SAPO-34 Membrane

Permeation data for CO<sub>2</sub>- CH<sub>4</sub> in a SAPO-34 membrane are shown in figure 8. The selectivity decreases with pressure drop but the CO<sub>2</sub> permeance remains reasonably constant so the best performance is obtained at low pressures. An extensive experimental study of this system together with detailed analysis of the experimental data according to the Maxwell-Stefan model was recently reported by Krishna et al<sup>(34)</sup>. For CO<sub>2</sub>-CH<sub>4</sub>, as well as for several other binary gas pairs in this membrane, mutual diffusion effects were insignificant so, to a reasonable approximation, the binary data could be represented by the Habgood model<sup>(55,56)</sup>. However, although the corrected diffusivity of CO<sub>2</sub> was almost independent of loading the corrected diffusivity of CH<sub>4</sub> showed a significant increase with loading (see figure 9a). In order to obtain a good representation of the binary data it was therefore necessary to allow for the concentration dependence of  $D_o$  (for CH<sub>4</sub>). This concentration dependence was correlated in accordance with the Reed – Ehrlich model<sup>(57)</sup>. A further refinement to the original Habgood model was the use of the simplified statistical isotherm<sup>(58)</sup> rather than the Langmuir isotherm, to calculate the chemical potential gradient. Representative results showing the comparison between the measured and predicted fluxes for both components in the binary system are shown in figure 9b. The agreement is excellent. Note that the lines for CO<sub>2</sub> and CH<sub>4</sub> are almost parallel, showing that, over this pressure range, the perm-selectivity does not vary much with pressure.

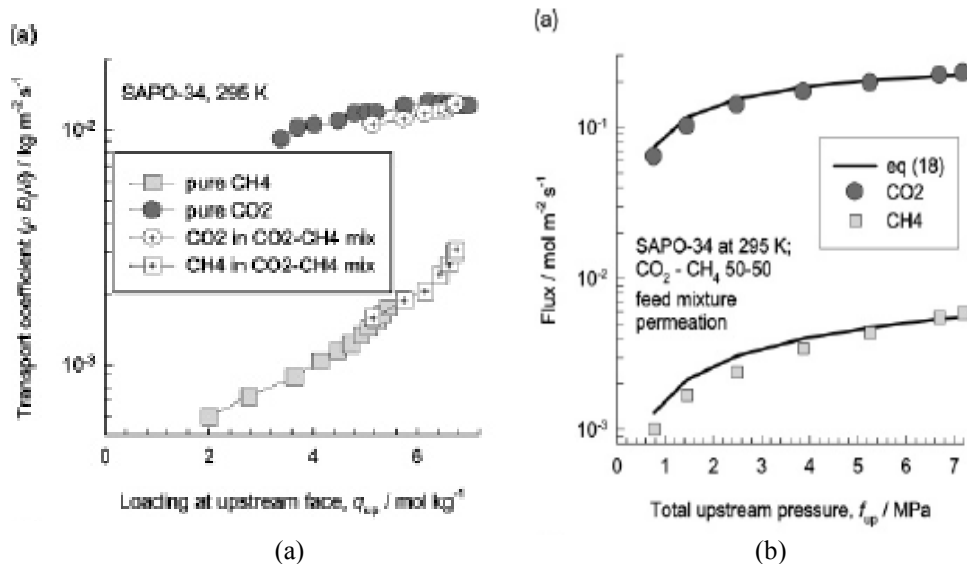


Fig. 9: Diffusion in SAPO-34: (a) Variation of corrected transport diffusivity ( $D_o/l$ ) for CO<sub>2</sub> and CH<sub>4</sub> in single component and binary systems. (b) Variation of flux with pressure for CO<sub>2</sub> and CH<sub>4</sub> in a binary system showing the comparison between experimental binary data and the predictions from single component data. From Li et al.<sup>(34)</sup>

### DDR-3 Membrane

The behavior of a DDR membrane (for CO<sub>2</sub>-CH<sub>4</sub>) is much less straightforward. Figure 10 shows the variation of the transport coefficients (directly proportional to the corrected diffusivities) extracted from the permeance data for the single components and binary mixtures reported by Himeno et al.<sup>(31)</sup> Very similar results have also been reported by van den Bergh et al.<sup>(59)</sup> Diffusion of CO<sub>2</sub> in the mixture is only slightly slower than in the single component system but the diffusivity of CH<sub>4</sub> in the mixture is substantially reduced with the result that the CO<sub>2</sub> selectivity is substantially greater than would be predicted simply from the ratio of the pure component permeances. The binary isotherm, as calculated from GCMC simulations, does not conform to the predictions of the ideal adsorbed solution theory (IAST), as may be seen from figure 11 and, regardless of the value used for the mutual diffusivity, it was not possible to reconcile the experimental permeance data with the Maxwell-Stefan model. Krishna and van Baten<sup>(60)</sup> and Sholl<sup>(61)</sup> have shown that these anomalies are due to preferential adsorption of CO<sub>2</sub> in the 8-ring windows of the DDR structure.

A detailed experimental study of diffusion of CO<sub>2</sub> and CH<sub>4</sub> in DDR crystals showed that, for both components, the diffusivities predicted by MD simulations using the standard (6-12) molecular potentials are about an order of magnitude too large. Jee and Sholl<sup>(61)</sup> have shown that a modified (6-18) potential can account correctly for both

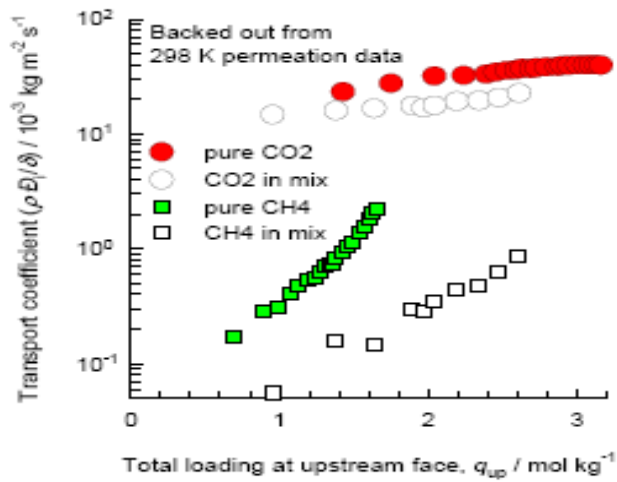


Fig. 10: Transport coefficients ( $\rho D_{0i}/\ell$ ) for CO<sub>2</sub> and CH<sub>4</sub> (as single components and in an equimolar binary mixture) extracted from permeance data for a DDR membrane. (Himeno et al<sup>(31)</sup>).

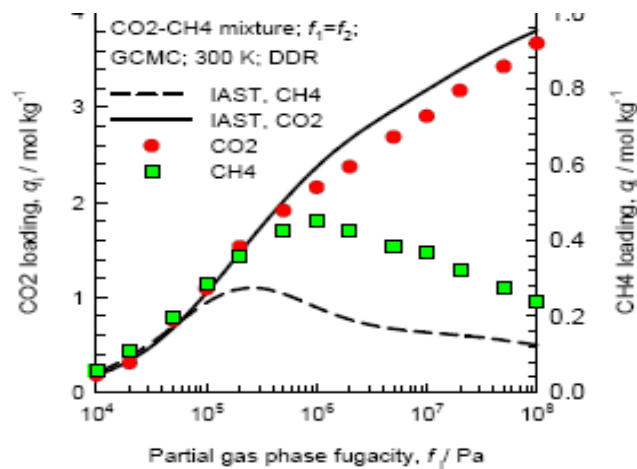


Fig. 11: Comparison of binary isotherms for CO<sub>2</sub>-CH<sub>4</sub> in DDR calculated by GCMC simulation and IAST. From Krishna and van Baten<sup>(60)</sup>.

the kinetic and equilibrium behavior. Representative results from these simulations are shown in figures 12 and 13, which include our limited experimental values. For the single component systems the trends are similar to those reported by Krishna and van Baten<sup>(60)</sup> (although quantitatively different). The significant reduction of the CH<sub>4</sub>

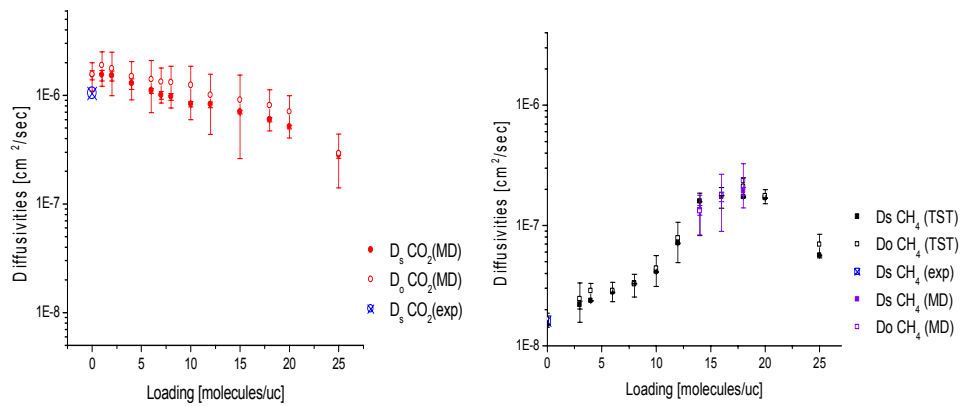


Fig. 12: Diffusion of CO<sub>2</sub> and CH<sub>4</sub> (as single components) in DDR-3 showing trends with loading and comparison with experimental data at low loading. Sholl<sup>(61)</sup>.

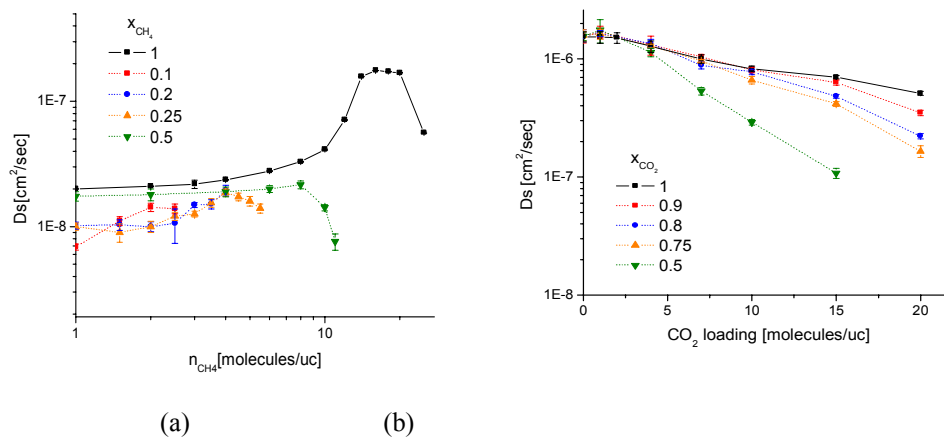


Fig. 13. Diffusion in DDR-3. (a) CH<sub>4</sub> in presence of CO<sub>2</sub>; (b) CO<sub>2</sub> in presence of CH<sub>4</sub>.

diffusivity with only a minor effect on the CO<sub>2</sub> diffusivity are correctly predicted. The dimensions of the 8-ring windows of SAPO-34 (3.8x4.3 Å) and DDR (3.65x4.35 Å) are similar but the minimum diameter of the DDR window is slightly smaller. It is remarkable that this small difference leads to such a difference in the diffusional behavior.

### Concluding Remarks

The three systems CH<sub>4</sub>-C<sub>2</sub>H<sub>6</sub>/ silicalite, CO<sub>2</sub>-CH<sub>4</sub>/SAPO-34 and CO<sub>2</sub>-CH<sub>4</sub>/ DDR-3 show different patterns of behavior that can be understood by considering the differences in pore size. The pores of silicalite are large enough for the light hydrocarbon molecules

to diffuse relatively freely without major energy barriers. In this situation mutual diffusion effects are significant since the interactions between the diffusing molecule are significant relative to the molecule pore interactions. In the smaller pores of SAPO-34 and DDR-3 the energy barrier associated with passage through the 8-rings is relatively large, so that the interactions between diffusing molecules becomes small in comparison with molecule-pore interaction, thus making mutual diffusion effects negligible. In DDR-3 the situation is further complicated by the tendency of the CO<sub>2</sub> molecules to sit preferentially in the windows, thereby obstructing the diffusion of CH<sub>4</sub> and enhancing the perm-selectivity for the mixture.

#### Appendix: Stefan Maxwell Formulation of the Ultrafiltration / RO Model

For a binary system the relationship between the flux and the gradient of chemical potential is given by Eq.17. In combination with Eq.3 this yields:

$$-\frac{N_i}{c_i} \left[ \frac{1}{D_{oi}} + \frac{X_j}{\mathcal{D}_j} \right] = \frac{dX_i}{dz} + X_i \left[ \frac{v_i}{RT} \frac{dP}{dz} - \frac{N_j}{\mathcal{D}_j c_i} \right] \quad (18)$$

In most R.O.and Ultrafiltration applications component i (the more permeable species) represents only a small fraction of the stream so  $X_j \rightarrow 1$ . Eq. 18 may therefore be integrated across the membrane to obtain:

$$\frac{N_i \ell}{c_i} \left[ \frac{1}{D_{oi}} + \frac{1}{\mathcal{D}_j} \right] = \frac{a [X_{iR} e^a - X_{iP}]}{e^a - 1} \quad (19)$$

where  $a = \frac{v_i \Delta P}{RT} + \frac{(N_i + N_j) \ell}{\mathcal{D}_j c_i}$ . Eq. 19 is obviously of the same form as Eq.5 with appropriately

modified diffusional resistance and parameter  $a_i$ .

#### Notation

$a$	$v \Delta P / RT$	$T$	temperature
$A$	$a D_{oi} c_{oi} / N_i \ell$	$v$	molar volume
$c$	fluid phase conc. (moles/m <sup>3</sup> )	$X$	mole fraction
$D$	diffusivity (m <sup>2</sup> s <sup>-1</sup> )	$z$	distance
$D_o$	corrected diffusivity	$\alpha$	separation factor
$D_K$	Knudsen diffusivity	$\gamma$	activity coefficient
$M$	molecular weight	$\varepsilon$	porosity
$N$	flux (mole/m <sup>2</sup> .s.)	$\mu$	chemical potential; viscosity
$P$	pressure (Pa)	$\mu^o$	standard chemical potential
$q$	adsorbed phase concentration	$\pi$	permeance (mole/m <sup>2</sup> .s.Pa)
$r$	mean pore radius; conc. ratio	$\Pi$	permeability (mole/m.s.Pa)
$R$	gas constant	$\tau, \tau^1$	tortuosity of membrane and support
$\Delta\pi$	osmotic pressure difference (Pa)		

## References

- [1] S.Sourirajan Reverse Osmosis, Academic Press, New York (1970).
- [2] C.T.Kresge, M.E.Leonowicz, W.J. Roth, J.C.Vartuli, and J.S.Beck Nature **359**, 710-712 (1992).
- [3] P.T.Tanev and T.Pinnavaia Chem.Mats. **8**, 2068, (1996)
- [4] M.Noack and J.Caro in Handbook of Porous Solids, F.Schueth, K.S.W.Sing and J.Weitkamp eds. Vol 4 p.2433 Wiley-VCH, Weinheim, Germany (2002)
- [5] J.G.Wijmans and R.W.Baker J. Membrane Sci. **107**, 1-21, (1995).
- [6] D.R.Paul J. Membrane Sci. **241**, 371-386, (2004).
- [7] C.J.Geankoplis, Transport Processes and Unit Operations 3rd ed. Ch. 12 p782 Prentice Hall, Englewood Cliffs, N.J. (1993).
- [8] C.Boissiere, M.U.Martines, A.Larbot and E.Prouzet J.Membrane Sci. **251**, 17-28, (2005)
- [9] C.Boissiere and M.U.Martines Chem. Mats. **15**, 460-463 (2003).
- [10] S. Bahtia, O. Jepps and D. Nicholson J.Chem.Phys. **120**, 4472-4485 (2004)
- [11] O.G. Jepps, S.K. Bahtia and D.J. Searles J.Chem.Phys. **119**, 1719-1730 (2003)
- [12] O.G.Jepps, S.K. Bahtia and D.J. Searles Phys.Rev.Letters **91**,126102 (2003)
- [13] S.K. Bahtia and D. Nicholson AIChEJ **52**, 29-38 (2006)
- [14] R. Krishna and J.M. van Baten Chem.Eng.Sci **64**, 870-882 (2009).
- [15] S.Higgins, W.DeSisto and D.M.Ruthven Microporous Mesoporous Mats.(2009)
- [16] D.M.Ruthven, W.J.DeSisto and S.Higgins Chem. Engg. Sci. (in press)
- [17] Q. Wei, Z. Nie, Y. Hao, J. Zou and W. Wang Materials Letters **59**, 3611-3615 (2005).
- [18] C. Li, J. Yang, X. Shi, J. Liu and Q. Yang Microporous and Mesoporous Materials **98**, 220-226 (2007).
- [19] C. Lesaint, B. Lebeau, C. Marichal and J. Patarin Microporous and Mesoporous Materials , **83**, 220-226 (2007).
- [20] Q. Wei, H.-Q. Chen, Z.-R. Nie, Y.-L. Hao, Y.-L. Wang, Q.-Y. Li and J.-X. Zou Materials Letters **61**, 1469-1473 (2007).
- [21] H.-M. Kao, J.-D. Wu, C.-C. Cheng and A.S. T. Chiang Microporous and Mesoporous Materials **88**, 319-328 (2006).
- [22] X. Wang, S. Cheng, J.C.C. Chan and J.C.H. Chao Microporous and Mesoporous Materials **96**, 321-330 (2006).
- [23] S. Fiorilli, B. Onida, B. Bonelli and E. Garrone J. Phys. Chem. B **109**, 16725-16729 (2005).
- [24] E. Maria Claesson and A.P. Philipse Colloids and Surfaces A: **297**, 46-54 (2007).
- [25] S. Higgins, R. Kennard, N. Hill, J. DiCarlo, and W.J. DeSisto, J.Membrane Sci. **279**, 669-674 (2006)
- [26] W.McBain, Sorption of Gases by Solids, Routledge, London (1932)
- [27] Prof. R.M. Barrer, Founding Father of Zeolite Science. British Zeolite Assoc.(1996)
- [28] R.Ash, R.M. Barrer and C.G. Pope Proc.Roy.Soc. A **271**, 1-18 (1963)
- [29] R.Ash, R.M.Barrer and R.T.Lowson J.J.Chem. Soc. Faraday Trans.1 **69**, 2166-2178 (1973).
- [30] M.B.Rao and S.Sircar Gas Separation and Purification **7**, 279-284 (1993)

- [31] S. Himeno, T. Tomita, K. Suzuki, K. Nakayama, K. Yajima and S. Yoshida, *Ind.Eng.Chem.Res.* **46**, 6989-6997 (2007). See also *Kagaku Kogaku Ronbun* **33**, 122 (2007).
- [32] J.van den Bergh, W. Zhu, J. Gascon, J.A. Moulijn and F. Kapteijn *J.Membrane Sci.* **316**, 35-45 (2008).
- [33] M.A. Carreon, S. Li, J.L. Falconer and R.D. Noble *J.Am.Chem.Soc.* **150**, 5412-5413, (2008).
- [34] S.Li, J.L.Falconer, R.D.Noble and R.Krishna *J.Phys.Chem.* **111**, 5075-5082 (2007)
- [35] S. Sridhar, R.S. Veerapur, M.B. Patil, K.B. Gudasi and T.M. Aminabhavi *J.App.Polymer Sci.* **106**, 1585-1594 (2007).
- [36] M. Iqbal, Z. Man, H. Mukhtar and B.K. Datta *J.Membr.Sci.* **368**, 167-175 (2008).
- [37] Y. Cai, Z. Wang, C. Yi, Y. Bai, J. Wang and S. Wang *J.Membr. Sci.* **360**, 184-196 (2008)
- [38] B. Ghalei and M.A. Semsarzadeh *Macromol.Symp.* 249-250 and 320-335 (2007)
- [39] J.Caro, M.Noack and P.Koelsch, *Adsorption* **11**, 215-227 (2005)
- [40] N.Hedin, G.J.DeMartin, K.G.Strohmaier and S.Reyes *Microporous Mesoporous Mats.* **98**, 182-188 (2007)
- [41] N.Hedin, G.J.DeMartin, W.J.Roth, K.G.Strohmaier and S.Reyes *Microporous Mesoporous Mats.* **109**, 327-334 (2008)
- [42] D.M.Ruthven and S.Reyes *Microporous Mesoporous Mats.* **104**, 59-66 (2007)
- [43] F.Kapteijn, J.A.Moulijn and R.Krishna *Chem.Engg. Sci.* **55**, 2923-2930, (2000)
- [44] F. J. Keil, R. Krishna and M-O. Coppens, *Rev. Chem. Eng.* **16**, 71-197 (2000).
- [45] R. Krishna, *Chem. Physics Letters* **326**, 477-484 (2000).
- [46] D. Paschek and R. Krishna, *Chem. Physics Letters* **333**, 278-284 (2001).
- [47] A.I. Skoulidas, D. S. Sholl and R. Krishna, *Langmuir* **19**, 7973-7988 (2003).
- [48] R.Krishna and R.Baur, *Sep. Purif. Technol.* **33**, 213-254, (2003).
- [49] R.Krishna and J.M.van Baten *J.Phys. Chem.B* **109**, 6386-6396, (2005)
- [50] R. Krishna and J. M. van Baten, *Chem. Eng. Technol.* **30**, 1235-1241 (2007).
- [51] R. Krishna and J. M. van Baten, *Chem. Physics Letters* **446**, 344-349 (2007).
- [52] R. Krishna, J. M. van Baten, E. Garcia-Perez and S. Calero, *Ind. Eng. Chem. Res.* **46**, 2974-2986 (2007).
- [53] R. Krishna, J. M. van Baten, *Microporous Mesoporous Mats.* **109**, 91-108 (2008).
- [54] J.M. van de Graaf, F.Kapteijn and J.Moulijn, *A.I.Ch.E.Jl* **45**, 497-511 (1999).
- [55] H. W. Habgood, *Can. J. Chem.* **36**, 1384-1397 (1958).
- [56] G. F. Round, H. W. Habgood and R. Newton, *Sep. Sci.* **1**, 219 (1966).
- [57] D.A.Reed and G.Ehrlich *Surf. Sci.* **102**, 588-609, (1981).
- [58] D.M.Ruthven *Principles of Adsorption and Adsorption Processes*, Ch. 3 and 4, John Wiley, New York, (1984)
- [59] J. van den Bergh, W.Zhu, J.Gascon, J.A.Moulijn and F.Kapteijn *J.Membrane. Sci.* **316**, 35-45, (2008).
- [60] R.Krishna and J.M. van Baten *Chem. Phys. Lett.* **446**, 344-349 (2007).
- [61] S.E Jee and D.Sholl, *J.Am.Chem.Soc* - submitted.
- [62] A.Markovic, D.Stoltenberg, D.Enke, E.U.Schluender and A.Seidel-Morgenstern *J.Membrane Sci.* - in press (2009)

**Acknowledgements:**

I am grateful to Prof. David Sholl for providing an advance copy of ref. 61 as well as for helpful discussions. Financial support of the National Science Foundation (GOALI program) is also gratefully acknowledged.